Hadronic Nucleus-Nucleus Cross Section and the Nucleon Size

Govert Nijs[1] and Wilke van der Schee[2]
[1]*Center for Theoretical Physics, Massachusetts Institute of Technology, Cambridge, Massachusetts 02139, USA*
[2]*Theoretical Physics Department, CERN, CH-1211 Genève 23, Switzerland*

(Received 3 August 2022; revised 10 October 2022; accepted 2 November 2022; published 29 November 2022)

Even though the total hadronic nucleus-nucleus cross section is among the most fundamental observables, it has only recently been measured precisely for lead-lead collisions at the LHC. This measurement implies the nucleon width should be below 0.7 fm, which is in contradiction with all known state-of-the-art Bayesian estimates. We study the implications of the smaller nucleon width on quark-gluon plasma properties such as the bulk viscosity. The smaller nucleon width dramatically improves the description of several triple-differential observables.

DOI: 10.1103/PhysRevLett.129.232301

Introduction.—The understanding of the creation quark-gluon plasma (QGP) as created at colliders such as the Large Hadron Collider (LHC) in Geneva requires the understanding of several stages of the collision of heavy ions [1,2]. The first stage is "far from equilibrium" and involves an initial condition together with an understanding of how this evolves toward a hydrodynamic QGP [3]. Second, there is a hydrodynamic stage, which involves understanding the temperature-dependent transport coefficients such as the shear viscosity [4]. Last, the QGP undergoes particlization into a gas of interacting hadrons that can then be detected experimentally.

Relatively little is known about the initial stage, for which the strongly coupled nature of QCD prohibits a full computation from first principles. In the high energy limit, progress can be made (see, e.g., Ref. [5]), but many state-of-the-art studies use a phenomenological parametrization of this initial stage. Here, a heavy ion is composed of a superposition of nucleons (208 for Pb) with Gaussian distributions of energy of width w. In principle the nucleon width can be measured. The charge radius equals 0.841 fm [6] and the two-gluon radius as measured by deep inelastic scattering by the HERA experiment equals 0.50 ± 0.03 fm [7] (see also Ref. [8]). The inelastic proton-proton hadronic cross section of $\sigma_{pp} = 68$ mb at $\sqrt{s} = 5.02$ TeV implies $r = 0.74$ fm in the black disk approximation, although σ_{pp} depends strongly on the collision energy $\sqrt{s}$.

A priori, it is, however, unclear that these measurements are directly related to the nucleon width within a nucleus as used in a model for the initial QGP. Hence, all Bayesian analyses so far have treated w as a phenomenological parameter. It is, however, important that independent of the width the nucleon-nucleon cross section σ_{NN} is fixed. This is achieved by having a w-dependent collision probability that effectively makes larger nucleons more transparent. Interestingly, all recent state-of-the-art global analyses of a wide variety of experimental data have preferred a large nucleon width in fm of 0.98 ± 0.18 [9], 0.96 ± 0.05 [10], 0.94 ± 0.18 [11], 1.05 ± 0.13 [12], or 0.82 ± 0.23 [13]. Since w equals the Gaussian width this implies that the resulting energy profile is then much larger than the charge radius.

In this Letter, we show that the recent ALICE measurement of the PbPb total hadronic cross section σ_{AA} of 7.67 ± 0.24 b at $\sqrt{s_{NN}} = 5.02$ TeV [14] implies a nucleon width smaller than approximately 0.7 fm, which is smaller than the width from all quoted Bayesian estimates. This measurement hence raises two important questions. First, why did the Bayesian probability estimates not result in the correct nucleon width? Second, what are the implications of this smaller nucleon width? Part of the answer to the first question must be an inaccurate estimate of the systematic uncertainty covariance matrix. Here, we note that the covariance matrix does not only include the systematic and statistical experimental and theoretical uncertainties, but it is essential to also include correlations or anticorrelations between observables. For the second question, the smaller nucleon width implies a larger bulk viscosity. Finally, we will show the improved analysis implies a better description of statistically difficult triple-differential observables.

Models that are inspired from first-principle arguments such as the IP-Glasma model [15] have always used a smaller nucleon width and then also turned out to have a relatively good description of the mentioned triple-differential observables [16,17]. In this way the new σ_{AA} measurement reconciles several puzzles in the field reconciles several puzzles in both the field of Bayesian analyses and on these more sophisticated observables.

The initial condition and the cross section.—All computations of σ_{AA} start with two nuclei that consist of a collection of nucleon positions. For this we use the point density distributions for both protons and neutrons from the recent implementation of Monte Carlo Glauber [18–21]. σ_{AA} is then determined by the condition that at least a single nucleon-nucleon interaction occurs.

In the black-disk approximation, nucleons interact if their distance d satisfies $d < \sqrt{\sigma_{NN}/\pi}$, with σ_{NN} the nucleon-nucleon cross section as determined from pp collisions at the same collision energy. In PYTHIA 8, a normalized overlap function is specified as a function of the impact parameter b as $T_{pp}(b) \propto \exp[-(b/w)^m]$ with w the nucleon width and $m = 1.85$ for the Monash tune [21,22]. In this Letter we will use the TRENTo model [23], which uses a Gaussian overlap function ($m = 2$) and the nucleon width w as a parameter. Nucleons then interact with probability $P(b) = 1 - \exp[-\sigma_{gg}\int d^2x_T T_A(x_T)T_B(x_T)]$, whereby σ_{gg} is determined by σ_{NN} [24]. The nucleons here are composed of smaller constituents (as in [9]), but we verified that this does not affect σ_{AA}.

It is no surprise that the (traditionally used) black-disk approximation produces the smallest σ_{AA}. Indeed, all models by construction have an equal nucleon-nucleon cross section, but wider overlap functions allow a nucleon-nucleon interaction to occur more easily for a nucleus-nucleus collision at relatively large impact parameter.

In Fig. 1, we see that σ_{AA} can increase up to 23% for w as large as 1.2 fm. Perhaps surprisingly, the dependence on σ_{NN} is fairly mild, and in this Letter we will keep the measured value of 61.2 and 67.6 mb for 2.76 and 5.02 TeV collisions, respectively [20]. The cross section depends linearly on the centrality normalization [13], e.g., on which events to count as a collision (as in the models above), or experimentally on how many collisions are recorded. Both theoretically and experimentally this contains an uncertainty, which we include as a separate parameter in Fig. 1 (bottom left). Motivated by [14], we give this parameter a prior probability distribution for our Bayesian analysis of a Gaussian with unit width. We note that this parameter propagates into a significant uncertainty, mainly for peripheral spectra and multiplicities but also for more central elliptic flow coefficients.

Crucially, σ_{AA} only depends sensitively on w, σ_{NN}, and the centrality normalization, whereby the latter two are well-constrained experimentally. A measurement of σ_{AA} hence provides robust constraints on w with only weak theoretical modeling uncertainties. The recently measured value of $\sigma_{AA} = 7.67 \pm 0.26$ b implies $w \approx 0.4$–0.5 fm (see Fig. 1), which, as noted in the introduction, is in direct contradiction with all state-of-the-art global analyses of heavy ion collisions so far.

Implications for QGP properties.—Figure 2 shows the posterior parameter analysis for the nucleon width w when including (left) or excluding (right) σ_{AA}. The unweighted red dashed fit is the result of a global analysis of 653 experimental data points [14,25–35] (see also the Supplemental Material [36]) with a 21-dimensional parameter space within the publicly available TRAJECTUM1.3 framework [37] similar to [11,13,38], but full details will be presented elsewhere [39]. TRAJECTUM translates the nucleon configurations into a QGP that evolves according to second order relativistic hydrodynamics until it particlizes into hadrons that are transported to the experimental detectors using the SMASH code [40–42]. (We will get back to the weighted and integrated curves shortly.) The analysis with σ_{AA} also includes the proton-lead cross section collisions at $\sqrt{s_{NN}} = 5.02$ TeV of $\sigma_{p\mathrm{Pb}} = 2.06 \pm 0.08$ b as measured earlier by CMS [35]. For this unweighted case, adding only these two experimental observations (σ_{AA} for PbPb [14] and pPb at 5.02 TeV [35,43]) indeed lowers the nucleon width from 0.98 ± 0.19 to 0.7 ± 0.14.

Nevertheless, from Fig. 1 we see that the nucleon width is still not quite compatible with the value required from the

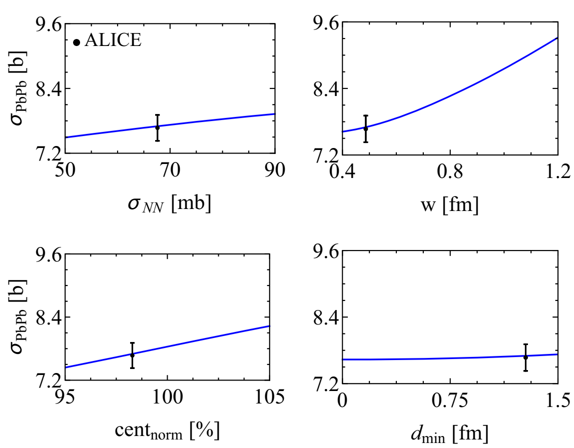

FIG. 1. We show the dependence of the PbPb cross section on the nucleon-nucleon cross section σ_{NN}, the nucleon width w, the centrality normalization cent$_{\mathrm{norm}}$, and the minimal nucleon-nucleon distance d_{min}. The parameters other than the one varied are kept fixed at the value indicated by the ALICE data point [14].

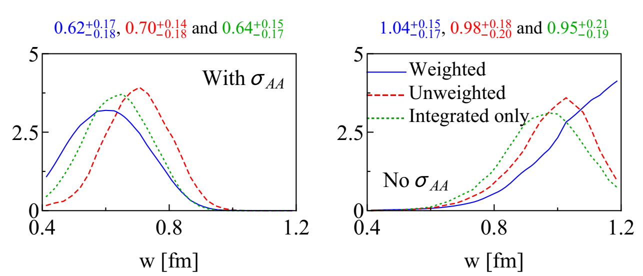

FIG. 2. We show posterior distributions for the nucleon width w with (left) and without (right) the new σ_{AA} measurement. For the fits we include all unweighted (red, dashed), all weighted (blue), and integrated only (green dotted) observables.

σ_{AA} measurement. This is consistent with the previous Bayesian analyses that strongly prefer larger widths and hence a Bayesian updated estimate now reduces the width, but not all the way to be compatible. Given the theoretical robustness of the σ_{AA} comparison, this remaining discrepancy has to be taken seriously. A crude way would be to fix $w = 0.45$ fm by hand or to use a prior distribution close to this value. A more quantitative approach is to give higher weights to observables we have a higher trust in on physical grounds, which is what we will attempt in this Letter.

Alternatively, we could say that the inconsistency of the nucleon width before and after σ_{AA} implies that we underestimated the systematic uncertainties. By far the best way would be to update those uncertainties, including, importantly, all (anti)correlations between all observables. In the current analysis data points from nearby bins are treated as correlated (see also Ref. [44]), although even here there is a certain level of arbitrariness. Moreover, there are theoretical uncertainties from, e.g., particlization that are even in principle hard to quantify. The weighting is a way to modify the relative importance of observable classes and hence correct for this uncertainty. This interpretation of extra uncertainty is more applicable to the theoretical uncertainty (where model uncertainties are hard to estimate), but we stress that even experimentally it is often not clear how all systematic uncertainties are correlated among observables.

As mentioned we highly trust σ_{AA} on the grounds that it is relatively model-independent theoretically and in fact only strongly depends on the nucleon width. Weaker but similar arguments can be made for integrated unidentified particle observables, such as integrated multiplicities, mean transverse momentum, and integrated anisotropic flow coefficients $v_n\{k\}$. Particle identified observables are theoretically more difficult to model and here we assign a weight 1/2. We define the weight ω to mean that we multiply the difference in an observable between theory and experiment by ω. Note that this preserves the correlation matrix. Also transverse momentum (p_T) differential observables are more model-dependent, especially at larger p_T, and similar arguments can be made for observables in peripheral centrality classes. We hence chose to weight p_T-differential observables by an extra factor 1/2 as well as an extra factor of $(2.5 - p_T[\text{GeV}])/1.5$ if $p_T > 1$ GeV. We also multiply the weight for any observable by $(100 - c[\%])/50$ if the centrality class c is beyond 50%.

The posteriors including the weights are shown in Fig. 2 as blue solid. Indeed by using lower weights for more model-dependent observables, we see the nucleon width is in agreement with the estimate from σ_{AA}. As shown in Table I, both including σ_{AA} and including weights improves the theoretical postdiction of σ_{AA} so that the agreement is within 1.1 (weighted) or 1.7 (unweighted) standard deviations of the ALICE result for PbPb and 1.5 and 1.9 standard deviations of the CMS result for pPb.

TABLE I. Posterior values for the PbPb and pPb cross sections for the four different fits compared to the ALICE [14] (PbPb) and CMS [35] (pPb) values. Theoretical emulation uncertainty is negligible and the uncertainty comes almost entirely from the posterior uncertainty on the nucleon width.

	σ_{PbPb} (b)	$\sigma_{p\mathrm{Pb}}$ (b)
σ_{AA} and weights	8.02 ± 0.19	2.20 ± 0.06
Weights	8.95 ± 0.36	2.48 ± 0.10
σ_{AA}	8.19 ± 0.19	2.25 ± 0.06
Neither	8.83 ± 0.29	2.45 ± 0.09
ALICE/CMS	7.67 ± 0.24	2.06 ± 0.08

Even though well-motivated, admittedly the weighting prescription has quite some arbitrariness. To verify the robustness of our results we also show the results of integrated only observables in Fig. 2. Since we put a lower weight on p_T-differential observables this could be seen as a more extreme version where such observables have zero weight. For the nucleon width and also for other all other parameters this does not lead to a significantly different posterior distribution. For pPb collisions, $\sigma_{p\mathrm{Pb}}$ should be a robust observable regardless of whether a hydrodynamic QGP description is valid for such small collision systems. Nevertheless, we also performed our analysis without including $\sigma_{p\mathrm{Pb}}$. This led to $w = 0.73 \pm 0.23$, so significantly larger than with pPb but still much smaller than without including σ_{AA}.

In Fig. 3, we show the temperature-dependent specific shear and bulk viscosities η/s and ζ/s with (blue) and without σ_{AA} (red). Given the smaller nucleon width, we expect a larger bulk and shear viscosity to reduce the average radial and elliptic flow that is induced by the larger

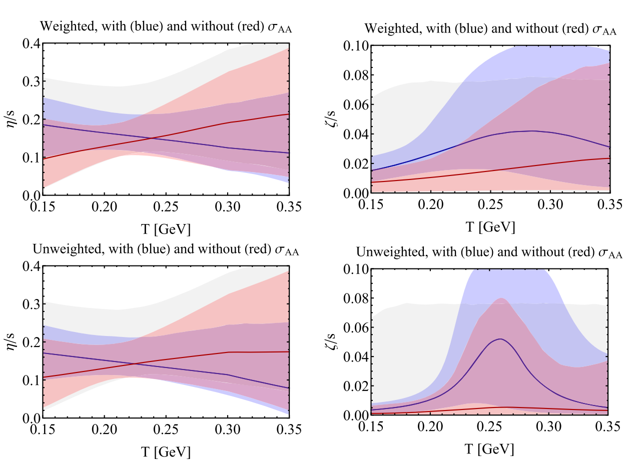

FIG. 3. We show the temperature-dependent specific shear and bulk viscosities η/s and ζ/s using the prior (gray) and posterior distributions from four different global analyses. This includes (blue) or excludes (red) σ_{AA}, and with (top) or without (bottom) weighting observables.

TABLE II. Average number of standard deviations from experimental data for different classes of observables for the four fits presented in Fig. 2 and the average weight $\bar{\omega}$ per observable class when used in the weighted analysis. Uncertainties include experimental uncertainty and theoretical uncertainty from the emulation (the latter is dominant for the v_n classes). Including the cross section σ_{AA} in the fit strongly improves the agreement with σ_{AA} but leads to only a mild worsening for the other observables.

	σ_{AA} and ω	ω	σ_{AA}	Neither	$\bar{\omega}$
$dN_{\mathrm{ch}}/d\eta$	0.55	0.60	1.23	1.22	1.00
$dN_{\pi^\pm,k^\pm,p^\pm}/dy$	0.76	0.70	0.60	0.57	0.48
$dE_T/d\eta$	1.59	1.51	0.82	0.77	0.48
$\langle p_T\rangle_{\mathrm{ch},\pi^\pm,K^\pm,p^\pm}$	0.66	0.60	0.88	0.72	0.46
$\delta p_T/\langle p_T\rangle$	0.56	0.62	0.51	0.58	0.49
$v_n\{k\}$	0.58	0.51	0.54	0.49	1.00
$d^2N_{\pi^\pm}/dydp_T$	1.19	1.07	0.86	0.92	0.20
$d^2N_{K^\pm}/dydp_T$	1.41	1.27	0.79	0.73	0.20
$d^2N_{p^\pm}/dydp_T$	1.35	1.21	0.73	0.67	0.25
$v_2^{\pi^\pm}(p_T)$	0.81	0.74	0.46	0.44	0.19
$v_2^{K^\pm}(p_T)$	0.92	0.89	0.55	0.55	0.19
$v_2^{p^\pm}(p_T)$	0.49	0.47	0.34	0.35	0.25
$v_3^{\pi^\pm}(p_T)$	0.65	0.57	0.69	0.57	0.24
average	0.89	0.83	0.69	0.66	
σ_{AA}	1.13	3.80	1.53	3.40	1.00

radial gradient. Interestingly, the nucleon width has a strong correlation with the slope of η/s, which is estimated to be negative with a 75% probability both for the weighted and unweighted distributions. Without including σ_{AA}, this probability is only 28%. We note that, without weighting, the bulk viscosity at low temperatures in particular has only a small uncertainty (bottom). In our view the uncertainty of the weighted result (top) is more realistic.

The nucleon width and observables.—After showing the σ_{AA} updated QGP properties, important questions remain. Why do analyses without σ_{AA} favor a large nucleon width, and is there an inconsistency given that the nucleon width is small? To answer these questions, Table II shows per class of observables the average discrepancy with the experimental result. Naturally, including the σ_{AA} dramatically improves the agreement with the σ_{AA} postdiction. What is, however, perhaps surprising is that the fit of the other observable classes only worsens mildly, on average worsening from 0.83 to 0.89 standard deviations for the weighted case. Virtually all observables get slightly worse, with the notable exception of the mean p_T fluctuations and $dN_{\mathrm{ch}}/d\eta$. Naturally, in the weighted case the observables with a lower weight have a worse agreement. We note that these deviations do not trivially translate into a χ^2 value since many observables are highly correlated (see also Ref. [44]). A more complete overview of the match of all observables is presented in the Supplemental Material [36], where indeed by eye it is difficult to see the difference between the fit with and without σ_{AA}.

An excellent test of our model is provided by the triple-differential observable $\rho(v_n\{2\}^2, \langle p_T\rangle)$, which measures the Pearson correlator between anisotropic flow and the mean p_T [45–47]. This observable is statistically expensive to compute (we simulate 625 000 hydro events for 20 parameter settings from the posterior) and hence cannot be included in the Bayesian fit. It moreover sensitively depends on the precise experimental procedure, including cuts on pseudorapidity, cuts on transverse momentum, and the method to select centrality bins [48]. Nevertheless, the observable is conjectured to be sensitive only to the hydrodynamic initial conditions, and in particular the nucleon width [49].

Figure 4 presents $\rho(v_n\{2\}^2, \langle p_T\rangle)$ as compared with ATLAS data [48]. Because of the expensive nature of this analysis, we only include systematic uncertainty from the posterior for the weighted case including σ_{AA} and show maximum *a posteriori* results for the unweighted with σ_{AA} and weighted without σ_{AA} cases. Clearly including σ_{AA} dramatically improves the description of this observable, which can at least in part be attributed to the smaller

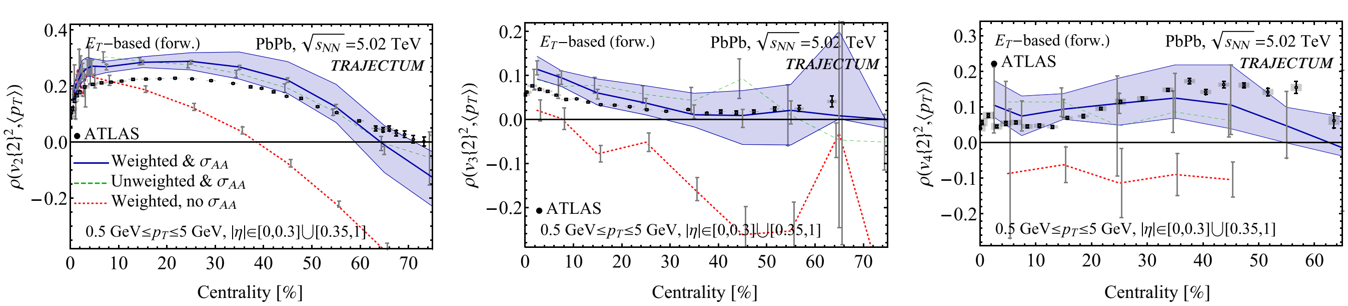

FIG. 4. We show the correlation between elliptic flow $v_2\{2\}^2$ (left), $v_3\{2\}^2$ (middle), and $v_4\{2\}^2$ (right) with mean transverse momentum $\langle p_T\rangle$ for weighted fit including (solid) and without (dotted) the cross section σ_{AA} and also the unweighted fit including σ_{AA} (dashed) for PbPb collisions. We show statistical uncertainties in gray and systematic uncertainties from the posterior as a band (first case only). We also include ATLAS data with systematic (boxes) and statistical uncertainties [48].

nucleon width [49]. A comparison with ALICE data [50] and XeXe collisions is included in the Supplemental Material [36].

Discussion.—A question deserving further study is in what way does our weighting procedure realistically capture the theoretical and experimental uncertainty? Indeed, systematic offsets on average observables are within 1 standard deviation of the experimental results and a naive χ^2 would say that the uncertainties are accurate (see also Table II and the Supplemental Material [36]). This, however, ignores the fact that the 653 data points are highly correlated, which is difficult to fully take into account. Also, while observables are on average 1 standard deviation away from the experimental results, the deviations are not Gaussian. Instead most observables are well within 1 standard deviation, while a small number deviate significantly. This is a further indication that a naive χ^2 should not be trusted. Nevertheless, all results presented are robust also without weighting, so that the naive uncertainty estimates also remain a viable option at the moment.

On a superficial level the results in this Letter show that the newly measured σ_{AA} improves estimates on the nucleon width, and subsequently the transport coefficients. We wish to caution here, however, that this fact should make us rethink the growing popularity of Bayesian analyses. Indeed, prior to this Letter all such analyses ruled out nucleon widths smaller than about 0.8 fm, which in light of this new analysis was not warranted. The question we should ask is does the data really convincingly imply such large nucleon widths?

In principle, given accurate estimates of the correlated uncertainties of the data and theoretical model, the Bayes posterior is accurate. Note, however, that even underestimating uncertainties by 10% is enough to cause an otherwise good fit to now be off by about 0.1 standard deviation, which, if this occurs for many data points, will add up, and the Bayesian analysis will try to compensate for this elsewhere. In a sense this means that the robustness of the Bayesian posterior depends sensitively on the accuracy of the uncertainty. We stress that the hardest part is to accurately estimate the theoretical model uncertainty. Currently this only includes emulation uncertainty, which can be sizeable but is not a physical uncertainty. Instead, many modeling choices such as our viscous particlization scheme (see Ref. [44]) or the particulars of the hadronic afterburner have uncertainties that are not included in the analysis. In fact, the full modeling uncertainty is difficult to quantify, though we note that the versatility of our 21-dimensional model attempts to include a wide scope of theoretical uncertainties.

It is perhaps curious that an early Bayesian study found a smaller width of 0.48 ± 0.1 [51,52]. As noted in [44], however, this is mostly due to having a simplistic initial stage where no radial flow is created during the first 0.4 fm/c and due to ignoring bulk viscous corrections during particlization. This earlier value is hence mostly a feature of the model being simplified, albeit in hindsight it produced a reasonable nucleon width estimate (but for the wrong reason).

Another relevant comment not included in this study is that the nucleon width could depend on the nucleons' position within the nucleus. It is not so unreasonable that nucleons in the skin of the nucleus could be smaller than nucleons in the center. The size of nucleons in the center would not significantly affect the nucleus-nucleus cross section.

We thank Somadutta Bhatta, Andrea Dainese, Giuliano Giacalone, Constantin Loizides, Aleksas Mazeliauskas, Rosi Reed, Mike Sas, Urs Wiedemann, and You Zhou for interesting discussions. G. N. is supported by the U.S. Department of Energy, Office of Science, Office of Nuclear Physics under Contract No. DE-SC0011090.

[1] U. Heinz and R. Snellings, Annu. Rev. Nucl. Part. Sci. **63**, 123 (2013).
[2] W. Busza, K. Rajagopal, and W. van der Schee, Annu. Rev. Nucl. Part. Sci. **68**, 339 (2018).
[3] J. Berges, M. P. Heller, A. Mazeliauskas, and R. Venugopalan, Rev. Mod. Phys. **93**, 035003 (2021).
[4] P. Romatschke and U. Romatschke, *Relativistic Fluid Dynamics In and Out of Equilibrium*, Cambridge Monographs on Mathematical Physics (Cambridge University Press, Cambridge, England, 2019).
[5] F. Gelis, E. Iancu, J. Jalilian-Marian, and R. Venugopalan, Annu. Rev. Nucl. Part. Sci. **60**, 463 (2010).
[6] R. Pohl *et al.*, Nature (London) **466**, 213 (2010).
[7] A. Caldwell and H. Kowalski, Phys. Rev. C **81**, 025203 (2010).
[8] B. Povh and J. Hufner, Phys. Rev. Lett. **58**, 1612 (1987).
[9] J. S. Moreland, J. E. Bernhard, and S. A. Bass, Phys. Rev. C **101**, 024911 (2020).
[10] J. E. Bernhard, J. S. Moreland, and S. A. Bass, Nat. Phys. **15**, 1113 (2019).
[11] G. Nijs, W. van der Schee, U. Gürsoy, and R. Snellings, Phys. Rev. Lett. **126**, 202301 (2021).
[12] D. Everett, W. Ke, J. F. Paquet, G. Vujanovic, S. A. Bass *et al.* (JETSCAPE Collaboration), Phys. Rev. C **103**, 054904 (2021).
[13] G. Nijs and W. van der Schee, Phys. Rev. C **106**, 044903 (2022).
[14] ALICE Collaboration, arXiv:2204.10148.
[15] B. Schenke, P. Tribedy, and R. Venugopalan, Phys. Rev. C **86**, 034908 (2012).
[16] G. Giacalone, B. Schenke, and C. Shen, Phys. Rev. Lett. **125**, 192301 (2020).
[17] ATLAS Collaboration, arXiv:2205.00039.
[18] B. Alver, M. Baker, C. Loizides, and P. Steinberg, arXiv: 0805.4411.
[19] C. Loizides, J. Nagle, and P. Steinberg, SoftwareX **1–2**, 13 (2015).
[20] C. Loizides, J. Kamin, and D. d'Enterria, Phys. Rev. C **97**, 054910 (2018); **99**, 019901(E) (2019).

[21] D. d'Enterria and C. Loizides, Annu. Rev. Nucl. Part. Sci. **71**, 315 (2021).
[22] P. Skands, S. Carrazza, and J. Rojo, Eur. Phys. J. C **74**, 3024 (2014).
[23] J. S. Moreland, J. E. Bernhard, and S. A. Bass, Phys. Rev. C **92**, 011901(R) (2015).
[24] To a good approximation, the scaling of the entropy deposited in the QGP is $\sqrt{T_A T_B}$.
[25] K. Aamodt *et al.* (ALICE Collaboration), Phys. Rev. Lett. **106**, 032301 (2011).
[26] J. Adam *et al.* (ALICE Collaboration), Phys. Rev. Lett. **116**, 222302 (2016).
[27] J. Adam *et al.* (ALICE Collaboration), Phys. Rev. C **94**, 034903 (2016).
[28] S. Acharya *et al.* (ALICE Collaboration), Phys. Lett. B **793**, 420 (2019).
[29] S. Acharya *et al.* (ALICE Collaboration), Phys. Rev. C **101**, 044907 (2020).
[30] B. Abelev *et al.* (ALICE Collaboration), Phys. Rev. C **88**, 044910 (2013).
[31] B. B. Abelev *et al.* (ALICE Collaboration), Eur. Phys. J. C **74**, 3077 (2014).
[32] S. Acharya *et al.* (ALICE Collaboration), J. High Energy Phys. 07 (2018) 103.
[33] J. Adam *et al.* (ALICE Collaboration), J. High Energy Phys. 09 (2016) 164.
[34] S. Acharya *et al.* (ALICE Collaboration), J. High Energy Phys. 09 (2018) 006.
[35] V. Khachatryan *et al.* (CMS Collaboration), Phys. Lett. B **759**, 641 (2016).
[36] See Supplemental Material at http://link.aps.org/supplemental/10.1103/PhysRevLett.129.232301 for an overview of all observables used together with the posteriors including and without the cross section as well as more results on the triple-differential observables.
[37] https://sites.google.com/view/govertnijs/trajectum.
[38] G. Nijs, W. van der Schee, U. Gürsoy, and R. Snellings, Phys. Rev. C **103**, 054909 (2021).
[39] G. Nijs and W. van der Schee, (to be published).
[40] J. Weil *et al.*, Phys. Rev. C **94**, 054905 (2016).
[41] D. Oliinychenko, V. Steinberg, J. Weil, M. Kretz, J. Staudenmaier, S. Ryu, A. Schäfer, J. Rothermel, J. Mohs, F. Li, H. E. (Petersen), L. Pang, D. Mitrovic, A. Goldschmidt, L. Geiger, J.-B. Rose, J. Hammelmann, and L. Prinz, smash-transport/smash: Smash-1.8 (2020).
[42] T. Sjostrand, S. Mrenna, and P. Z. Skands, Comput. Phys. Commun. **178**, 852 (2008).
[43] B. B. Abelev *et al.* (ALICE Collaboration), J. Intrum. **9**, P11003 (2014).
[44] J. E. Bernhard, Bayesian parameter estimation for relativistic heavy-ion collisions, Ph.D. thesis, Duke U., 2018.
[45] P. Bozek, Phys. Rev. C **93**, 044908 (2016).
[46] P. Bozek and H. Mehrabpour, Phys. Rev. C **101**, 064902 (2020).
[47] G. Giacalone, F. G. Gardim, J. Noronha-Hostler, and J.-Y. Ollitrault, Phys. Rev. C **103**, 024909 (2021).
[48] ATLAS Collaboration, arXiv:2205.00039.
[49] G. Giacalone, B. Schenke, and C. Shen, Phys. Rev. Lett. **128**, 042301 (2022).
[50] S. Acharya *et al.* (ALICE Collaboration), Phys. Lett. B **834**, 137393 (2022).
[51] J. E. Bernhard, J. S. Moreland, S. A. Bass, J. Liu, and U. Heinz, Phys. Rev. C **94**, 024907 (2016).
[52] G. Giacalone, arXiv:2208.06839.